

DESY 83-023
March 1983



THE ARGUS ELECTRON/PHOTON CALORIMETER

II) PROPERTIES OF THE LIGHT COLLECTION SYSTEM

OF THE LEAD/SCINTILLATOR SHOWER COUNTERS

by

A. Drescher, H.J. Graf, B. Gräwe, W. Hofmann,
A. Markees, U. Matthiesen, J. Spengler, D. Wegener

Institut für Physik der Universität Dortmund

ISSN 0418-9833

NOTKESTRASSE 85 · 2 HAMBURG 52

DESY behält sich alle Rechte für den Fall der Schutzrechtserteilung und für die wirtschaftliche Verwertung der in diesem Bericht enthaltenen Informationen vor.

DESY reserves all rights for commercial use of information included in this report, especially in case of filing application for or grant of patents.

To be sure that your preprints are promptly included in the
HIGH ENERGY PHYSICS INDEX,
send them to the following address (if possible by air mail) :

DESY
Bibliothek
Notkestrasse 85
2 Hamburg 52
Germany

THE ARGUS MUON CHAMBERS

A.Arefiev, M.Danilov, Yu.Gorodkov, V.Lubimov,
Yu.Semenov, V.Tchistilin, I.Tichomirov, Yu.Zaitsev

Institute of Theoretical and Experimental Physics, Moscow, USSR

ABSTRACT

The performance of the ARGUS muon chambers is reported. The proportional tube characteristics are described and some test results are presented.

INTRODUCTION

The new universal detector ARGUS has been built for the study of electron-positron interactions at the DORIS II storage ring [1]. The detector is equipped with three layers of muon chambers (fig.1). The chambers are designed to detect charged particles (mostly muons) which penetrate an absorber formed by the shower counters, copper coils and iron flux return yoke of the magnet. One layer of chambers is installed inside the magnet 3.3 absorption lengths from the interaction point and covers 43% of the full solid angle. Two layers of the chambers outside the yoke (1.8 absorption lengths) cover 87% of the full solid angle (with 93% overlapping). The presence of such absorbers leads to momentum cuts of about 700 MeV/c and 1100 MeV/c for muons detected by the inner and outer chambers respectively.

Due to a small counting rate it is rather difficult to monitor the muon chamber efficiency. That is why they were thoroughly constructed and tested before the installation. In this paper we describe the muon chamber design, the test procedure and the actual performance.

CHAMBER DESIGN

A single chamber consists of eight proportional counters (tubes) glued together and welded to aluminium plates at both ends (fig.2). The plates are provided with holes for mounting. A high voltage power supply board, a preamplifier connector, a high voltage connector, and a gas inlet and outlet are attached to one of the aluminium plates. A chamber length was determined by the magnet dimensions, and the chamber location in the detector. The length ranges from 1 to 4 meters.

Each counter was made from an extruded rectangular aluminium tube of an internal cross-section $56 \times 56 \text{ mm}^2$ and 2 mm wall thickness. A $50 \mu\text{m}$ gold plated tungsten wire stretched with a tension of 1.5 N was positioned in the center of the tube with an accuracy of $\pm 0.3 \text{ mm}$. The wire was crimped into a thin brass tube which was epoxyed in the center of the plastic end cap, which was also supplied with a gas inlet. These end caps were glued into the aluminium tubes with silicon rubber thus providing gas tight volumes for each counter.

The gas amplification G for a counter depends on the high voltage HV , the gas density ρ and the argon-methane volume ratio m :

$$\delta C/C = \kappa_1 \delta HV/HV + \kappa_2 \delta \rho/\rho + \kappa_3 \delta m/m \quad (1)$$

The measured gas amplification as a function of the high voltage is shown in fig.3 for two argon-methane mixtures. The dependence of the signal amplitude on gas pressure is shown in fig.4 for the mixture (92%Ar+8%CH₄). According to these two pictures the values of the constants in eq.(1) for such a counter at a temperature of $T=20^\circ\text{C}$ and a voltage of $HV = 2.35 \text{ kV}$ are as follows

$$\kappa_1 = 23, \quad \kappa_2 = -4, \quad \kappa_3 = 1.4$$

To minimize the background it is preferable to use a gas with a high drift velocity. The nonflammable gas mixture (92%Ar+8%CH₄) was chosen primarily for safety reasons.

If one approximates a rectangular tube by a cylinder of 65 mm diameter, the dependence of the gas amplification on the variation of the tube radius R , on the wire radius r , and on the displacement d of the wire from the geometrical center will be:

$$\delta C/C = -\kappa_1 / \ln(R/r) \cdot \delta R/R = -3 \delta R/R$$

$$\delta C/C = -[1 - \kappa_2 - \kappa_1 / \ln(R/r)] \cdot \delta r/r = -2 \delta r/r$$

$$\delta C/C = \kappa_1 \cdot [(d/R)^2 / \ln(R/r) + 2\pi d/R^2] = 3 \cdot 10^{-2} (d^2 + 0.4 \cdot d)$$

The actual value $\delta r/r = 10^{-2}$ leads to $\delta C/C = 2\%$. The mechanical tolerances of the counter dimensions of $\delta R/R \leq 2 \cdot 10^{-3}$ correspond to $\delta C/C = 0.5\%$. Amplitude variations due to gravitational displacement of a 4-meter long sense wire or its centering do not exceed $\delta C/C \leq 1\%$. Thus the chamber construction leads to an uncertainty of the gas amplification of about 3% which does not influence the detection of particles in a threshold mode.

TESTING PROCEDURE

The system of 250 chambers (2000 counters) was built at ITEP and transported from Moscow to Hamburg by truck. Before transportation all chambers underwent a preliminary test. A chamber passed the test if:

1. the dark current of a chamber filled with nitrogen did not exceed the value of $2 \cdot 10^{-8} \text{ A}$ at $HV = 3 \text{ kV}$,
2. the pressure drop velocity did not exceed $10^{-2} \text{ torr-liter}\cdot\text{sec}^{-1}$ for a chamber filled with helium at 40 torr above the local atmospheric pressure.

3. the sense wire tension did not differ by more than 10% from the calculated value as was checked by measuring the resonance frequency of the wire under a current in a magnetic field.

At DESY the resonance frequency was measured once more to check the wire tension.

The leakage of a single chamber was less than $2 \cdot 10^{-3}$ torr \cdot sec $^{-1}$ at a pressure of about 10 torr. Thus the leakage for all the chambers with a total volume of $V=20.5$ m 3 was 0.15 liter \cdot min $^{-1}$.

The counter detection efficiency and the drift velocity have been measured in the 2 GeV electron beam at DESY. The typical efficiency dependence on high voltage for a single counter is shown in fig.5. The total spread in the rising part of this curve for all counters was about 100 V and a working voltage 2.35 kV was chosen. The chamber efficiency dependence on the beam position is presented in fig.6. The arrows at this figure indicate the boundaries of a single counter.

The drift time-space relation is shown in fig.7. The straight lines in this figure correspond to a drift velocity of $V_{dr}=5$ cm/ μ sec. At this drift velocity the minimum gate width for the electronics has to be of the order of 0.8 μ sec to ensure efficiency for the whole counter. This value fits well with the DORIS II bunch repetition time of 0.96 μ sec. The efficiency along the wire was measured with cosmic particles to determine the effective longitudinal dimension of the chambers. The efficiency drops to 50% at a distance of 1.4 cm from the counters edge.

The final test was the measurement of an amplitude spectrum with cosmic particles for each counter though only hit information is used in the experiment. A simplified block diagram of the test set-up for amplitude measurements of four chambers simultaneously is shown in fig.8. The cosmic particle trigger was provided by a coincidence of signals from scintillation counters located above and below the chambers.

Before every measurement all amplitude channels were calibrated automatically. The typical amplitude spectrum for a single counter is shown in fig.9. For each counter the mean amplitude and dispersion of these spectra were calculated. The spread of these values for all counters was within $\sigma = \pm 5\%$. The signal amplitudes from the middle of a 4-meter long counter and from its ends coincide to within 1%. The single counter rates from cosmic rays were within $\pm 10\%$ relative to the average value of $N_0 = 28$ sec $^{-1}$ \cdot m $^{-1}$.

To check on the long time operation the block of 48 4-meter long chambers with the electronics, readout and gas systems was tested during half a year. The block diagram of readout electronics for one channel is shown in fig.10 (see more in detail [2]). The system was triggered when a signal amplitude from any of 384 counters was greater than 1 mV. Periodically the single counting rates of each tube were measured. The deviation from the mean counting rate for these chambers, corrected for

atmospheric pressure variations is shown in fig.11. As indicated by this figure the chambers show a stability of 1% over a long time period.

ACTUAL PERFORMANCE

A total of 218 muon chambers (1744 tubes) of seven different lengths were mounted on the ARGUS detector in August 1982. These chambers were used in the run of October-December 1982. The whole system has operated in a stable and reliable manner since the very beginning. A typical event of the type $e^+e^- \rightarrow \mu^+\mu^-$ at a c.m. energy $\sqrt{S} = 10$ GeV is shown in fig.12. One can see the clean signals in the muon chambers. The background counting rate was rather low. The average number of hits was 0.98 /event.

During the runs careful attention was paid to the control of all muon chamber components, as it was impossible to get an efficiency estimation from on line procedures. Systematically a hit distribution per trigger and a wire map were checked. The readout electronic system was tested with a pulse generator controlled by a computer which measured a threshold distribution for all channels. The gas quality was checked with eight proportional counters which were irradiated by the radioactive source Fe 55 .

The efficiency of the muon chambers was obtained in an off line analysis from the cosmic data by tracing tracks from the drift chamber. The average efficiency per layer for all chambers was $\epsilon = 0.978 \pm 0.001$.

All the tests and measurements discussed in this paper have shown that the ARGUS muon chambers are adequate for the purpose of muon detection.

ACKNOWLEDGEMENTS:

We wish to thank all those at ITEP who contributed to the construction of the muon chambers, particularly D.Barskii, V.Bocharov, B.Gordeev, G.Divulskii, A.Mileshkin, and also V.Sopov and V.Tchernyshev who participated in the muon chamber installation and operation.

We thank the DESY personnel who helped us during the tests of the muon chambers and the installation of them in ARGUS. We are indebted to the members of the DESY group F 51 for their help.

Those of us who worked at DESY wish to thank the DESY authorities for their hospitality.

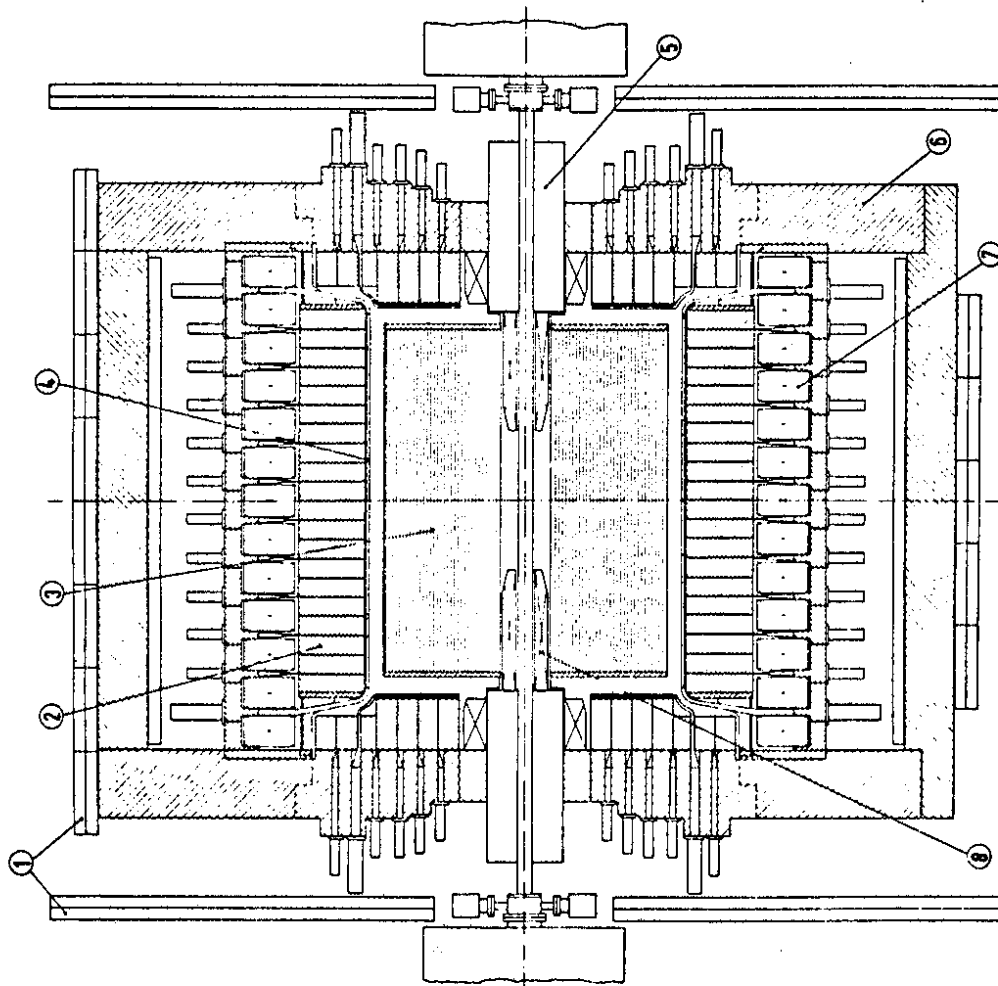
FIGURE CAPTIONS.

- Fig.1. The ARGUS detector.
- Fig.2. The muon chamber schematic view.
- Fig.3. The gas amplification as a function of the high voltage for two argon-methane mixtures.
- Fig.4. The dependence of the sense wire amplitude (in channels) on the gas pressure.
- Fig.5. The typical operating plateau.
- Fig.6. The chamber efficiency dependence on the electron beam position.
- Fig.7. The drift time-space relation.
- Fig.8. The muon chamber test set-up.
- Fig.9. The amplitude spectrum for a single counter (in channels).
- Fig.10. The block diagram of readout electronics.
- Fig.11. Deviation of the chamber counting rate from the mean value.
- Fig.12. A typical $e^+e^- \rightarrow \mu^+\mu^-$ event at a c.m.s. energy 10 GeV.

REFERENCES

- [1] H.Hasemann et al. ARGUS. A new detector for DORIS. Int. Rep. DESY F15/Pro148, October 1978.
- [2] H.Brechtel, H.J.Stuckenberg. Int. Rep. DESY F56-72/1, October 1972.
W.Neff, H.J.Stuckenberg, G.Will. Int. Rep. DESY F56-72/2, October 1972.

ARGUS Detector



- 1. Muon chambers
- 2. Shower counters
- 3. Drift chamber
- 4. Time of flight counters
- 5. Mini beta quadrupole
- 6. Iron yoke
- 7. Solenoid coils
- 8. Compensation coils

FIG. 1

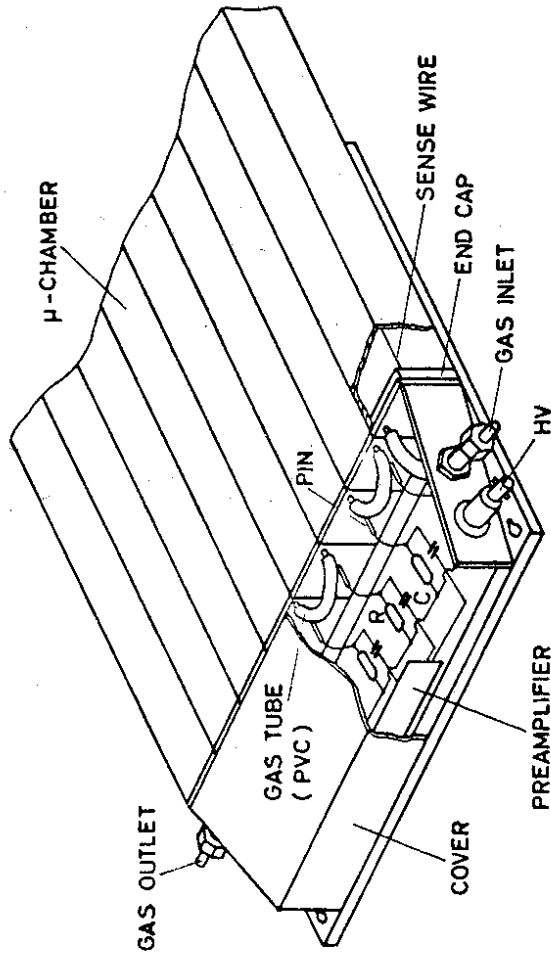


FIG. 2

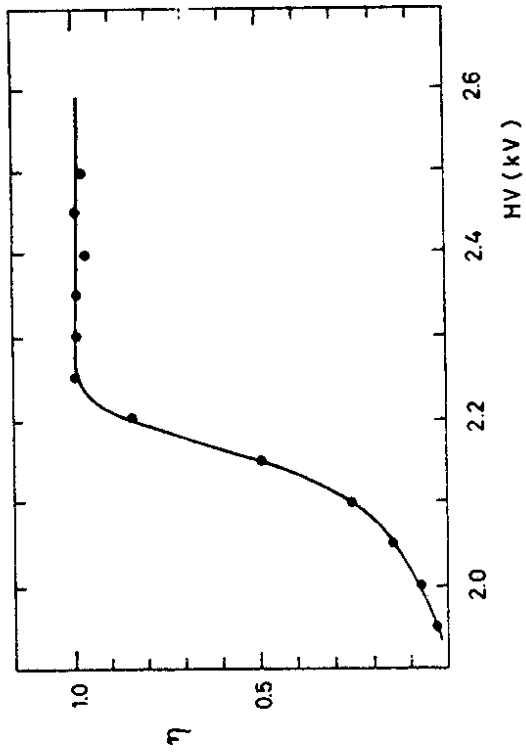


FIG. 5

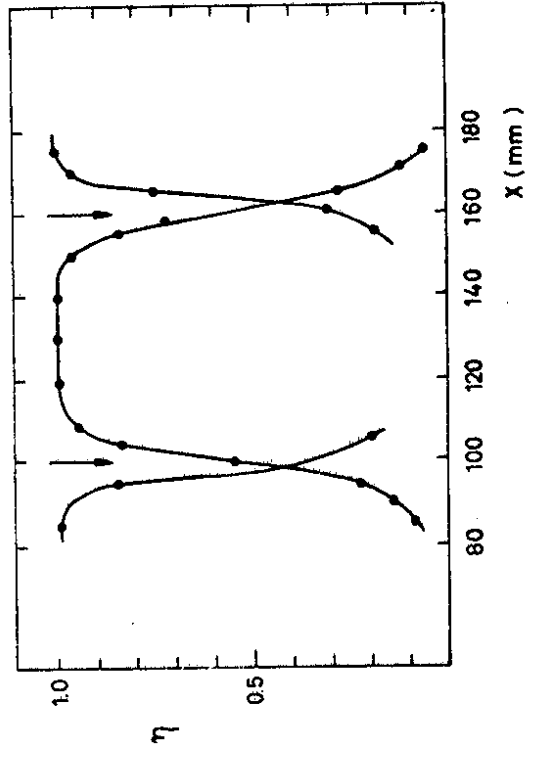


FIG. 6

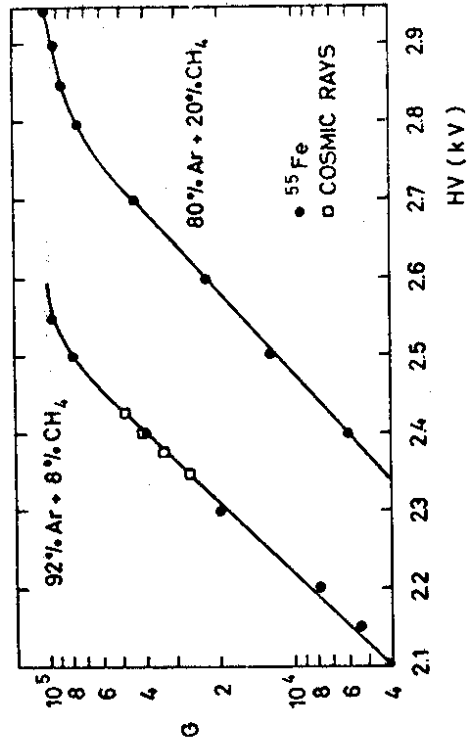


FIG. 3

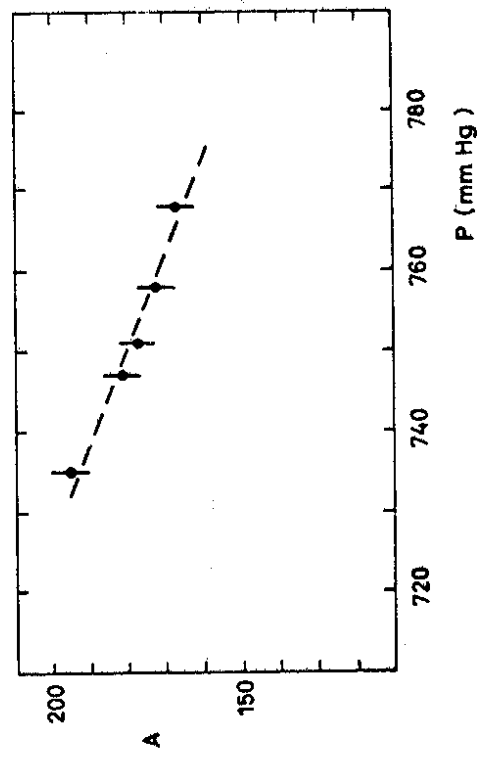


FIG. 4

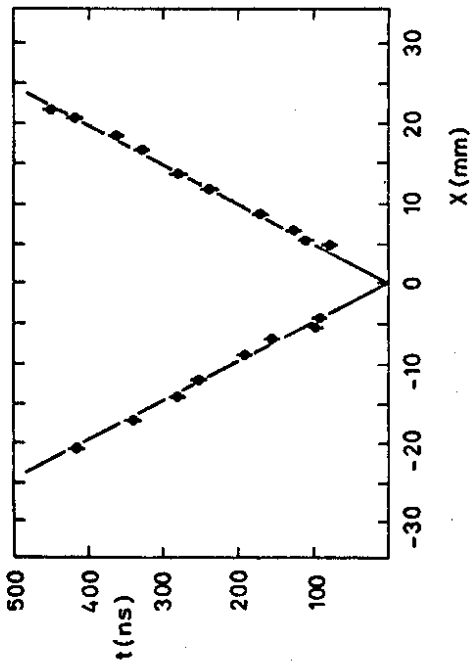


FIG. 7

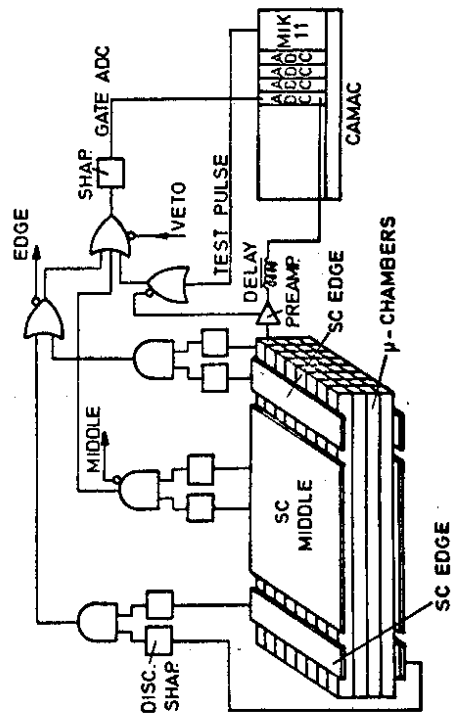


FIG. 8

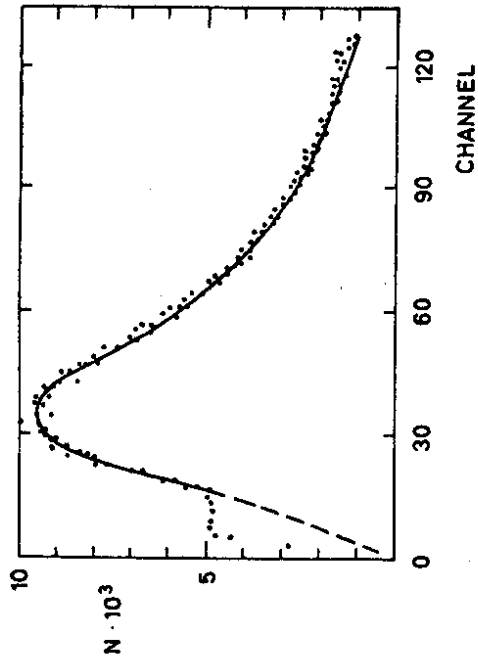


FIG. 9

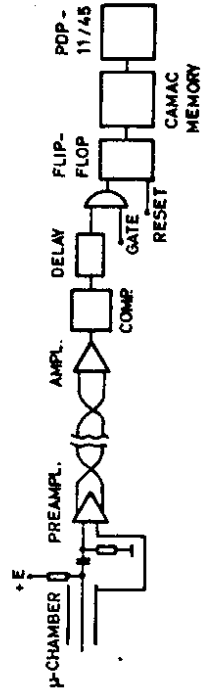


FIG. 10

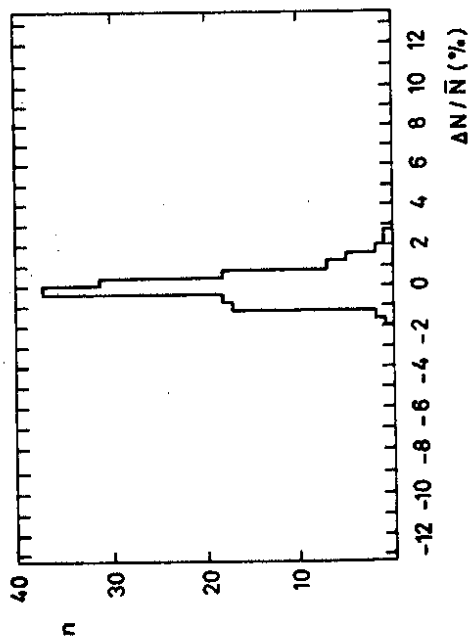


FIG. 11

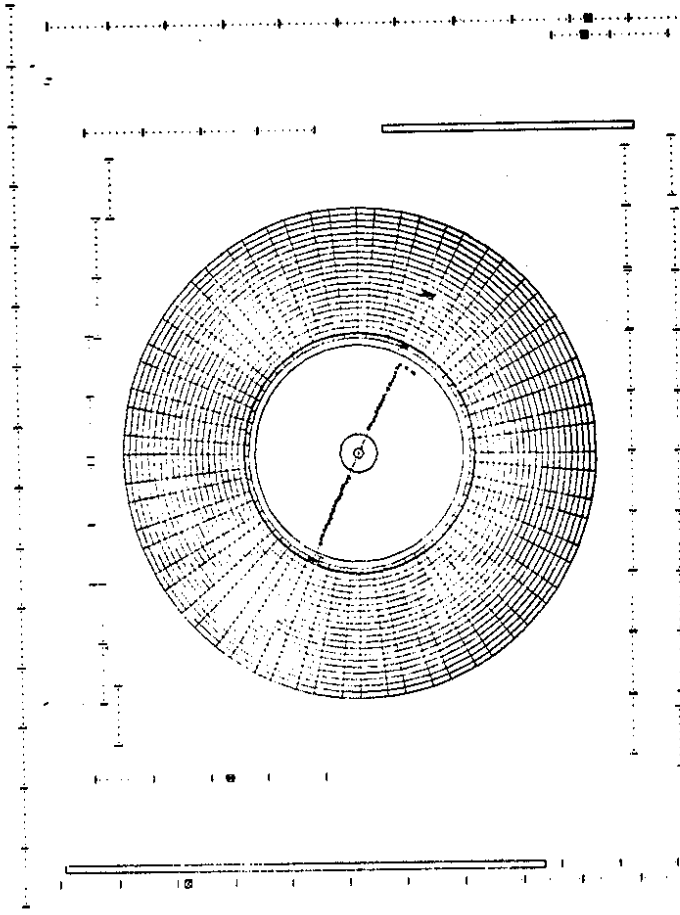


FIG. 12